SYNODIC AND SIDEREAL ROTATION PERIODS OF KORONIS FAMILY MEMBER (1762) RUSSELL

Stephen M. Slivan, Abigail Colclasure, Inés Escobedo, Aidan Henopp, Rory Knight, Andi Mitchell
Massachusetts Institute of Technology,
Dept. of Earth, Atmospheric, and Planetary Sciences
77 Mass. Ave. Rm. 54-427, Cambridge, MA 02139
slivan@mit.edu

Francis P. Wilkin
Union College Dept. of Physics and Astronomy
Schenectady, NY

(Received: 2021 November 10)

Rotation lightcurves of Koronis asteroid family member (1762) Russell were observed in 2021, yielding a synodic rotation period of 12.7946 ± 0.0004 h. The precision is shown to be sufficient to unambiguously count sidereal rotations across the entire data set of available Russell lightcurves, and constrain the sidereal rotation period to 12.79381 ± 0.00007 h prograde.

Koronis family member (1762) Russell was observed in 2021 as part of an ongoing observing program to study rotation properties of the family's brighter objects (Slivan et al., 2008). Previous lightcurve observations of Russell from 2014 have been reported by Cooney et al. (2015), spanning 44 days with a derived rotation period of 12.797 ± 0.007 h. Subsequent statistical analyses of "sparse data" from photometric surveys have produced solutions for sidereal periods and pole locations that are not consistent with each other within their estimated errors (Ďurech et al., 2018a; Ďurech and Hanuš, 2018b). The new observations were made to improve the determination of the synodic rotation period, by obtaining a set of lightcurves spanning a relatively long calendar interval of several lunations during the 2021 apparition (Slivan, 2012).

Nightly observing information is summarized in Table I, and details about the instruments used are given in Table II. Observations prior to the Sep. 8 opposition were made using telescopes at the Wallace Astrophysical Observatory in Westford, MA. Processing and measurement of the images were as described by Slivan et al. (2008), except that for these observations made using smaller telescopes the choices of synthetic aperture sizes for the on-chip relative photometry were guided by the experience of Howell (1989). Observations near and after opposition were made remotely using the CHI-1 telescope of Telescope Live in Rio Hurtado, Chile, for which candidate nights during the post-opposition lunation were identified specifically to overlap the best pre-opposition coverage of rotation phase. The CHI-1 images were measured using *AstroImageJ*, and comparison stars having APASS DR10 catalog colors similar to solar were used to minimize systematic errors in the zero-point calibration to r' magnitudes.

The calibrated r' data were reduced to unit distances. A fit of the Lumme-Bowell model (Bowell et al., 1989) to the brightnesses of the well-observed lightcurve maximum was used to determine the slope parameter of $G_{r'} = 0.285$ used to account for changing solar phase angle in producing the composite lightcurve (Fig. 1).

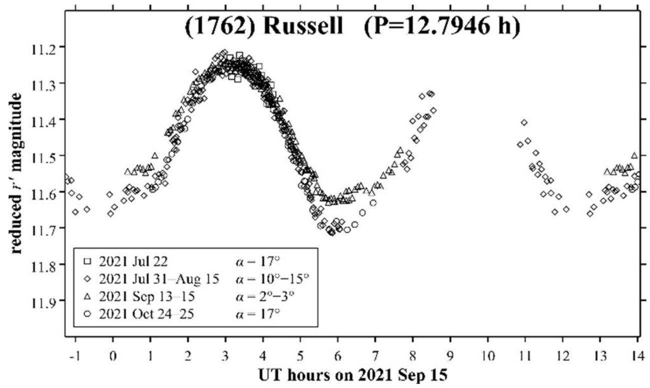

Figure 1. Folded composite lightcurve of (1762) Russell during four lunations of its 2021 apparition, light-time corrected, showing one rotation period plus the earliest and latest 10% repeated. The estimated error in the r' zero-point calibration is 0.03 mag. Nights of relative photometry have been shifted in brightness to form a self-consistent composite with the calibrated r' lightcurves. Solar phase angles α of the observations are given in the legend, and changing depth of the lightcurve minima with solar phase angle is apparent.

The best information to improve the period comes from the observations on Jul. 31 and on Oct. 25, which recorded the same rotation phase brightness increase and lightcurve maximum 86 days apart at comparable solar phase angles. The derived synodic period 12.7946 ± 0.0004 h is consistent with the previously published synodic period.

The "sieve algorithm" of Slivan (2013) is used here to test whether the improved period precision is sufficient to unambiguously count sidereal rotations across the entire available lightcurve data set. In addition to the lightcurves from 2014 and 2021, observations of Russell made in 2019 and 2020 by the ATLAS astrometric survey (Tonry et al., 2018) are suitable for folded composite lightcurves and are publicly available online from the MPC astrometry Web site; the epochs measured for all four apparitions are given in Table III.

The initial constraint on the sidereal period for the algorithm is based on the best synodic period, but at the precision level of the new determination, the change in viewing aspect during the time interval spanning the observations upon which it is based also is significant and needs to be accounted for. Instead of dividing the time interval by the integer number of elapsed synodic rotations N, a range of sidereal periods allowing for the maximum possible effect of the aspect change is calculated by using $N \pm (\Delta\lambda_{PAB}/360°)$ as the divisor where $\Delta\lambda_{PAB}$ is the change in ecliptic longitude of the phase angle bisector. In this case $N = 161$ rotations and $\Delta\lambda_{PAB} = 3.5°$ allowing a range of possible sidereal periods up to 0.0008 h shorter and longer than the synodic period, which when combined with 2.5× the period error to include a ~99% confidence interval, yields an initial constraint range half-width of 0.0018 h. The algorithm results (Fig. 2) confirm an unambiguous solution that corresponds to 5202 sidereal rotations during the maximum epoch interval, leaving unknown only the sign of the fractional part that depends on the direction of spin.

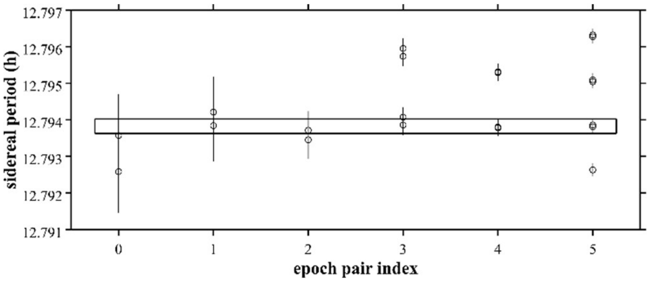

Figure 2: Single range of possible sidereal rotation periods of (1762) Russell allowed by the epochs in Table III as described in the text. The epoch measurement adopted errors are 28 min which is 1.5× the maximum observed asymmetry of the timing of the maxima in the composite lightcurves. Each horizontal coordinate index marks the time interval between a pair of epochs, with longer intervals to the right. Open circles and vertical bars represent sidereal periods and period ranges, respectively, calculated from every possible number of rotations that could elapse during the interval. The thin horizontal rectangle identifies the single range of periods that is allowed by all six time intervals.

Distinguishing between the two corresponding possible sidereal period ranges - one each prograde and retrograde, overlapping - requires knowing the direction of spin. Although the available data do not confidently fully locate the pole, there is enough information for sidereal photometric astrometry (Slivan, 2014; Drummond et al., 1988) to identify prograde rotation, for which the corresponding allowed range for the sidereal period from the sieve algorithm is 12.79363 to 12.79399 h. Adopting the associated period result from the algorithm, with the allowed range as an estimate of a ~99% confidence interval (half-width 2.5σ), yields a sidereal period of 12.79381 ± 0.00007 h prograde. The period result is consistent with that of Ďurech et al. (2018a) but not Ďurech and Hanuš (2018b).

UT date 2021	Tel. ID	Filter	Solar phase angle(°)	PAB λ (°)
Jul 22.2	WAO-4	*R*	17.2	343.8
Jul 31.3	WAO-3	*R*	14.9	344.6
Aug 01.2	WAO-3,4	*R*	14.7	344.7
Aug 03.2	WAO-3	*R*	14.1	344.9
Aug 07.2	WAO-2	*R*	12.9	345.1
Aug 14.2	WAO-2,4	*R*	10.5	345.5
Aug 15.3	WAO-2,3	*R*	10.1	345.6
Sep 13.1	CHI-1	*r′*	1.9	346.0
Sep 14.2	CHI-1	*r′*	2.4	346.0
Sep 15.1	CHI-1	*r′*	2.8	346.0
Oct 24.1	CHI-1	*r′*	16.6	348.0
Oct 25.1	CHI-1	*r′*	16.9	348.1

Table I: Nightly observing information, with rows grouped by lunation. Columns are: UT date at lightcurve mid-time, telescope ID (see Table II), filter used (Cousins R; Sloan r'), solar phase angle, and J2000 ecliptic longitude of the phase angle bisector.

Tel. ID	Dia. (m)	CCD camera	FOV (′)	Bin	Scale (″/pix)	Int. (s)
WAO-2	0.36	SBIG STL-1001	22×22	1×1	1.26	180
WAO-3	0.36	SBIG STL-1001	20×20	1×1	1.18	180
WAO-4	0.36	SBIG STL-1001	21×21	1×1	1.25	180
CHI-1	0.61	FLI-PL9000	32×32	2×2	1.24	240

Table II: Telescopes and cameras information. Columns are: telescope ID, telescope diameter, CCD camera, detector field of view, image binning used, binned image scale, and image integration time used.

UT epoch	PAB λ,β(°)	Data reference
2014 Mar 23 1.23 h	164.4 +0.3	Cooney et al. 2015
2019 Mar 14 1.46 h	174.7 +0.7	ATLAS-MLO *o*-band
2020 May 31 5.29 h	253.0 +2.8	ATLAS-MLO *o*-band
2021 Oct 25 2.76 h	348.1 -0.8	this paper

Table III: Summary of (1762) Russell lightcurve epochs, in each case locating a maximum from the second harmonic of a Fourier series model that was fit to lightcurves. λ,β are J2000 ecliptic longitude and latitude of the phase angle bisector. Photometry from the ATLAS-MLO survey (Tonry et al., 2018) was retrieved from the MPC Orbits/Observations Database.

Acknowledgements

We thank Dr. Michael Person and Timothy Brothers for allocation of telescope time at Wallace and for observer instruction and support. The student observers were supported by a grant from MIT's Undergraduate Research Opportunities Program. We thank Ernesto Guido at Telescope Live for very timely assistance with the remote observing. F. Wilkin received funding from the Faculty Research Grant at Union College. This work has made use of the AAVSO Photometric All-Sky Survey (APASS), funded by the Robert Martin Ayers Sciences Fund and NSF AST-1412587. This work also has made use of data and services provided by the International Astronomical Union's Minor Planet Center; specifically, the brightnesses accompanying astrometry from the Asteroid Terrestrial-impact Last Alert System (ATLAS) survey observing program.

References

Bowell, E.; Hapke, B.; Domingue, D.; Lumme, K.; Peltoniemi, J.; Harris, A.W. (1989). "Application of Photometric Models to Asteroids." In *Asteroids II* (R.P. Binzel; T. Gehrels; M.S. Matthews, eds.) pp. 524-556. Appendix: The IAU Two-Parameter Magnitude System for Asteroids. U. of Arizona Press, Tucson, AZ.

Cooney, W.R.; Gross, J.; Terrell, D.; Klinglesmith, D.A.; Hanowell, J. (2015). "Rotation Period and Lightcurve of 1762 Russell." *Minor Planet Bull.* **42**, 66–67.

Drummond, J.D.; Weidenschilling, S.J.; Chapman, C.R.; Davis, D.R. (1988). "Photometric geodesy of main-belt asteroids. II. Analysis of lightcurves for poles, periods, and shapes." *Icarus* **76**, 19-77.

Number	Name	yyyy mm/dd	Phase	L_{PAB}	B_{PAB}	Period(h)	P.E.	Amp	A.E.
1762	Russell	2021 07/22-10/25	*17.2,16.9	346	0	12.7946	0.0004	0.46	0.03

Table IV. Observing circumstances and results. Solar phase angle is given for the first and last dates; the asterisk indicates that the phase angle reached a minimum within that interval. L_{PAB} and B_{PAB} are the phase angle bisector longitude and latitude at mid-date range.

Ďurech, J.; Hanuš, J.; Alí-Lagoa, V. (2018a). "Asteroid models reconstructed from the Lowell Photometric Database and WISE data." *Astron. Astrophys.* **617**, A57.

Ďurech, J.; Hanuš, J. (2018b). "Reconstruction of asteroid spin states from Gaia DR2 photometry." *Astron. Astrophys.* **620**, A91.

Howell, S.B. (1989). "Two-dimensional Aperture Photometry: Signal-to-noise Ratio of Point-source Observations and Optimal Data-extraction Techniques." *PASP* **101**, 616-622.

Slivan, S.M.; Binzel, R.P.; Boroumand, S.C.; Pan, M.W.; Simpson, C.M.; Tanabe, J.T.; Villastrigo, R.M.; Yen, L.L.; Ditteon, R.P.; Pray, D.P.; Stephens, R.D. (2008). "Rotation Rates in the Koronis Family, Complete to $H \approx 11.2$." *Icarus* **195**, 226-276.

Slivan, S.M. (2012). "Epoch Data in Sidereal Period Determination. I. Initial Constraint from Closest Epochs." *Minor Planet Bull.* **39**, 204-206.

Slivan, S.M. (2013). "Epoch Data in Sidereal Period Determination. II. Combining Epochs from Different Apparitions." *Minor Planet Bull.* **40**, 45-48.

Slivan, S.M. (2014). "Sidereal Photometric Astrometry as Efficient Initial Search for Spin Vector." *Minor Planet Bull.* **41**, 282-284.

Tonry, J.L.; Denneau, L.; Heinze, A.N.; Stalder, B.; Smith, K.W.; Smartt, S.J.; Stubbs, C.W.; Weiland, H.J.; Rest, A. (2018). "ATLAS: A High-cadence All-sky Survey System." *PASP* **130**, 064505.

PHOTOMETRIC OBSERVATIONS AND DATA ANALYSIS OF NEA BINARY ASTEROID 5143 HERACLES

Brian D. Warner
Center for Solar System Studies / MoreData!
446 Sycamore Ave.
Eaton, CO 80615 USA
brian@MinorPlanetObserver.com

Robert D. Stephens
Center for Solar System Studies / MoreData!
Rancho Cucamonga, CA 91730

(Received: 2022 January 12)

Analysis of CCD photometric observations of the known binary asteroid 5143 Heracles (Taylor et al., 2012) was conducted at the Center for Solar System Studies based on observations obtained in 2021 October and November. A secure period of P1 = 2.70776 ± 0.00006 h was established for the rotation of the primary. The secondary period is ambiguous and depends on whether or not the rotation of the secondary is locked to its orbital period. Our analysis favors an independently rotating secondary with P2 = 46.41 h.

Observations of the near-Earth asteroid 5143 Heracles were made at the Center for Solar System Studies in 2021 October and November. They were made with a 0.35-m f/9.1 Schmidt-Cassegrain and FLI Microline CCD camera. The camera uses a KAF-1001E chip, which has a 1024×1024×24m array of pixels. The combination gives a field-of-view of about 25×25 arcminutes and image scale of 1.5 arcsec/pixel. The analysis of our data follows below.

All lightcurve observations were unfiltered since a clear filter can cause a 0.1-0.3 mag loss. The exposure duration varied depending on the asteroid's brightness and sky motion. Guiding on a field star sometimes resulted in a trailed image for the asteroid.

Measurements were made using *MPO Canopus*. The Comp Star Selector utility in *MPO Canopus* found up to five comparison stars of near solar-color for differential photometry. To reduce the number of adjusted nightly zero points and their amounts, the analysis of the 2021 data used the ATLAS catalog r´ (SR) magnitudes (Tonry et al., 2018). The rare zero-point adjustments ≥ ±0.03 mag may be related in part to using unfiltered observations, poor centroiding of the reference stars, not correcting for second-order extinction, or selecting a star that is an unresolved pair.

The Y-axis values are ATLAS SR "sky" (catalog) magnitudes. The two values in the parentheses are the phase angle (a) and the value of *G* used to normalize the data to the comparison stars used in the earliest session. This, in effect, corrected all the observations to seem to have been made at a single fixed date/time and phase angle, leaving any variations due only to the asteroid's rotation and/or albedo changes. The X-axis shows rotational phase from -0.05 to 1.05. If the plot includes the amplitude, e.g., "Amp: 0.65", this is the amplitude of the Fourier model curve and *not necessarily the adopted amplitude for the lightcurve*.

References to previous works were taken from the asteroid lightcurve database (Warner et al., 2009), known as "LCDB" from here on. Since most listed rotation periods for the primary were very similar, only a few of the LCDB references have been used.